Available online at www.sciencedirect.com

ScienceDirect

Ceramics International 37 (2011) 1569–1573

CERAMICS INTERNATIONAL

www.elsevier.com/locate/ceramint

# A comparative study on combustion synthesis of Ta–B compounds

C.L. Yeh *, H.J. Wang

*Department of Aerospace and Systems Engineering, Feng Chia University, 100 Wenhwa Rd., Seatwen, Taichung 40724, Taiwan*

Received 10 November 2010; received in revised form 1 December 2010; accepted 13 January 2011
Available online 18 February 2011

## Abstract

A comparative study on the preparation of various tantalum borides (including $Ta_2B$, $Ta_3B_2$, TaB, $Ta_5B_6$, $Ta_3B_4$, and $TaB_2$) in the Ta–B system was experimentally conducted by self-propagating high-temperature synthesis (SHS) from the elemental powder compacts of their corresponding stoichiometries. Both combustion temperature and reaction front velocity increased and then decreased with increasing boron content in the powder mixture. The fastest flame front with a reaction temperature of 1732 °C and a propagation rate of 11.2 mm/s was observed in the sample of Ta:B = 1:1. The combustion temperature (1205 °C) and flame-front velocity (3.82 mm/s) for the powder compact of Ta:B = 2:1 were the lowest. According to the XRD analysis, single-phase TaB and $TaB_2$ were produced from the samples of Ta:B = 1:1 and 1:2, respectively. However, multiphase products were synthesized from the samples of other stoichiometries. In the final products from Ta-rich samples of Ta:B = 2:1 and 3:2, two boride phases, $Ta_2B$ and TaB, along with a large amount of residual Ta were detected. The products yielded from boron-rich reactants of Ta:B = 5:6 and 3:4 were composed of TaB, $Ta_3B_4$, and $TaB_2$. Based upon the temperature dependence of combustion wave velocity, the activation energies associated with the formation of TaB and $TaB_2$ by solid state combustion were determined to be 131.1 and 181.4 kJ/mol, respectively.

*Keywords:* Tantalum boride; Self-propagating high-temperature synthesis (SHS); Activation energy; X-ray diffraction

## 1. Introduction

Borides of several transition metals in groups IVB and VB, such as $TiB_2$, $ZrB_2$, $HfB_2$, and $TaB_2$, are members of a family of materials known as ultra high-temperature ceramics. In addition to high melting temperatures, they have a unique combination of high hardness, high electrical and thermal conductivities, chemical stability, good thermal shock resistance, and excellent corrosion resistance [1–4]. Potential applications of these transition metal borides include thermal protection components, cutting tools, refractory crucibles, impact-resistant armors, and plasma-arc electrodes [3,4]. However, tantalum borides have not been studied as extensively as other borides, like $TiB_2$ [1,5], $ZrB_2$ [2,3], and $HfB_2$ [2,6]. According to the Ta–B phase diagram [7], there are five boride phases including $Ta_2B$, $Ta_3B_2$, TaB, $Ta_3B_4$, and $TaB_2$. Besides, a new phase $Ta_5B_6$ and its crystal structure were later identified by Bolmgren et al. [8].

On the formation of tantalum borides, a variety of processing routes have been utilized. For example, Hideaki et al. [9] produced $TaB_2$, TaB, and $Ta_3B_4$ by solid state reactions of mixed Ta and amorphous boron powders under corresponding compositions at 800, 900, and 1800 °C, respectively. Peshev et al. [10] obtained $TaB_2$ through borothermic reduction of $Ta_2O_5$ at 1650 °C for 1 h. The diboride $TaB_2$ with comparable mechanical properties to $ZrB_2$ and $HfB_2$ was also fabricated by reducing $Ta_2O_5$ with $B_4C$ and graphite at 1600 °C [2]. As a promising alternative, combustion synthesis in the mode of self-propagating high-temperature synthesis (SHS) takes advantage of the self-sustaining merit from highly exothermic reactions, and therefore, has the benefits of low energy requirement, short reaction time, and simple facilities [11–14]. Production of transition metal borides by the SHS process is typically through the direct reaction of constituent elements in a sample compact, by which many borides including $TiB_2$, $ZrB_2$, $HfB_2$, $NbB_2$, and NbB were synthesized [15–20]. Furthermore, a large number of composites based upon transition metal borides, such as $TiB_2$–TiC, $TaB_2$–TaC, $TaB_2$–SiC, $TiB_2$–AlN, $NbB_2$–$Al_2O_3$, and $TiB_2$–mullite, have been produced by self-sustaining combustion involving metallic elements and $B_4C$, BN, or $B_2O_3$ [21–26].

---

* Corresponding author. Tel.: +886 4 24517250x3963; fax: +886 4 24510862.
*E-mail address:* clyeh@fcu.edu.tw (C.L. Yeh).

0272-8842/$36.00
doi:10.1016/j.ceramint.2011.01.024

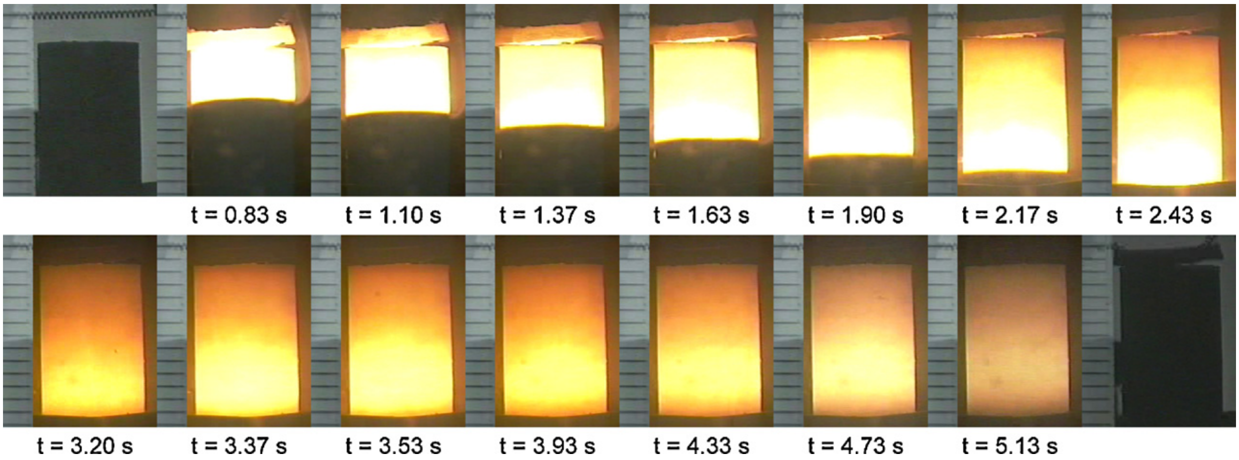

Fig. 1. A sequence of recorded images illustrating self-sustaining combustion of a Ta + 2B powder compact diluted with 3.5 mol% of $TaB_2$.

In spite of the existence of six boride phases in the Ta–B system, the diboride $TaB_2$ has been the focus of attention for most of the previous work. Therefore, this study aims to investigate the feasibility of preparing various tantalum borides by the SHS process using the elemental powder compacts of their corresponding stoichiometries. Not only the phase composition of the final product but also the combustion temperature and flame-front velocity of the sample compact studied. In addition, the apparent activation energies associated with the formation of specific tantalum borides were deduced by correlating the dependence of flame-front velocity on combustion temperature.

## 2. Experimental methods of approach

Tantalum (Aldrich, <45 μm, 99.9% purity) and amorphous boron (Noah Technologies Corp., 1 μm, 92% purity) powders were used as the starting materials of this study. Powder blends with six different atomic ratios including Ta:B = 2:1, 3:2, 1:1, 5:6, 3:4, and 1:2 were prepared in a ball mill. Mixed powders were then cold-pressed into the cylindrical sample compact with a diameter of 7 mm, a height of 12 mm, and a compaction density relative to 45% of the theoretical maximum density (TMD). The SHS experiments were conducted in a stainless-steel windowed chamber under an atmosphere of high purity argon (99.99%). In the experiment, a compressed pellet made up of Ti and carbon powders with Ti:C = 1:1 was placed on the top of the reactant compact to serve as an ignition enhancer which was triggered by a heated tungsten coil. Details of the experimental setup and measurement approach were reported elsewhere [20,22]. The phase constituent of the synthesized product was identified by an X-ray diffractometer (Shimadzu XRD-6000) with $CuK_\alpha$ radiation. Furthermore, boride compounds, TaB and $TaB_2$, fabricated in this study were adopted as the diluents to mix with elemental Ta and B powders for determination of the activation energy of the reaction.

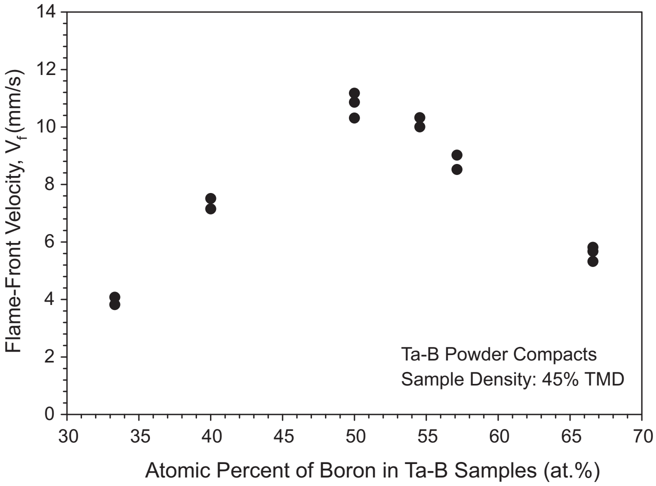

Fig. 2. Effect of starting stoichiometry of Ta–B powder compacts on flame-front propagation velocity.

## 3. Results and discussion

### 3.1. Measurement of flame-front velocity and combustion temperature

Experimental evidence of this study showed that solid state combustion of the powder compact with or without boride dilution was characterized by a nearly planar reaction front traversing the entire sample in a self-sustaining manner. A typical SHS sequence is illustrated in Fig. 1, where a Ta + 2B sample diluted with 3.5 mol% of $TaB_2$ is presented. As revealed in Fig. 1, the reaction front reached the bottom of the sample at about $t = 2.43$ s and a distinct afterburning glow appears from $t = 3.37$ s. This implies that the phase transformation is not only restricted to the combustion front, but also continues volumetrically after the passage of the reaction front.

Based upon the recorded combustion images, the flame-front propagation velocity ($V_f$) along the powder compact was determined. The flame velocity of the undiluted sample was found to be significantly affected by the starting stoichiometry. With the increase of the atomic percent of boron in the Ta–B powder compact, Fig. 2 indicates that the reaction front velocity increases, reaches a maximum of 11.2 mm/s at 50 at.% of boron

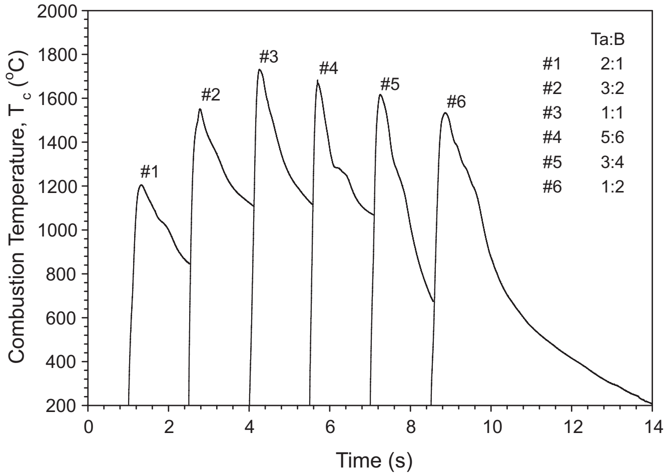

Fig. 3. Typical combustion temperature profiles of Ta–B powder compacts with different stoichiometric proportions.

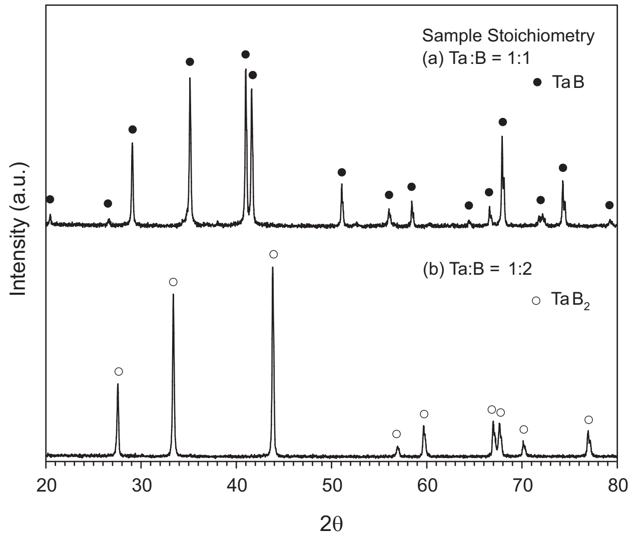

Fig. 4. XRD patterns of final products synthesized from powder compacts with (a) Ta:B = 1:1 and (b) Ta:B = 1:2.

(i.e., Ta:B = 1:1), and then decreases. The slowest reaction front with $V_f = 3.82$ mm/s was observed in the Ta-rich sample of Ta:B = 2:1, which represents the composition with the lowest content of boron. On the other hand, for the composition with the highest content of boron (i.e., Ta:B = 1:2), the flame speed of about 5.6 mm/s was detected. The composition dependence of the combustion velocity is most likely attributed to the variation of reaction exothermicity with different stoichiometry of the sample.

Fig. 3 depicts six representative temperature profiles recorded from combustion of the powder compacts with different initial compositions. The abrupt rise in the temperature curve signifies the rapid arrival of the combustion wave. The peak temperatures corresponding to the reaction front temperatures varied between 1205 and 1732 °C. Most importantly, the composition dependence of the combustion wave temperature is consistent with that of the flame-front velocity shown in Fig. 2.

### 3.2. *Phase constituents of combustion products*

The XRD analysis indicated that only TaB and $TaB_2$, as presented respectively in Fig. 4(a) and (b), were produced in the pure form from the samples of their equivalent stoichiometries. For the samples of other starting compositions, the XRD patterns of their resulting products are plotted in Fig. 5. In addition to $Ta_2B$ and TaB, Fig. 5(a) and (b) shows that the final products obtained from two Ta-rich samples of Ta:B = 2:1 and 3:2 contain a large amount of residual Ta. This implies an incomplete phase conversion, due probably to the relatively low reaction temperatures for these two samples and the insufficient reaction time typical of the SHS process. It should be noted that for the sample of Ta:B = 3:2, the dominant boride was TaB and the amount of $Ta_2B$ was trivial, but no $Ta_3B_2$ was detected in its resulting product.

The XRD patterns of the final products obtained from the samples rich with boron at Ta:B = 5:6 and 3:4 are respectively depicted in Fig. 5(c) and (d), both of which show a mixture of three boride phases, including TaB, $Ta_3B_4$, and $TaB_2$. Specifically, TaB dominates over $Ta_3B_4$ and $TaB_2$ in the product synthesized from the sample of Ta:B = 5:6. For the product from the sample of Ta:B = 3:4, both TaB and $TaB_2$ are considered as the major constituents and $Ta_3B_4$ as the minor. Similar to the case of Ta:B = 3:2, Fig. 5(c) shows the absence of $Ta_5B_6$ in spite of the green compact starting at Ta:B = 5:6. This might suggest that $Ta_3B_2$ and $Ta_5B_6$ are kinetically unfavorable

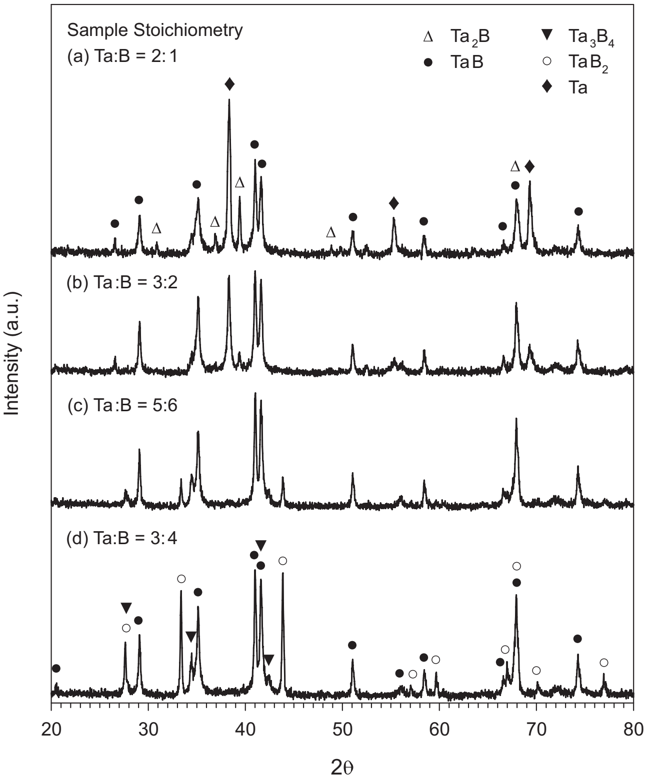

Fig. 5. XRD patterns of final products synthesized from powder compacts with (a) Ta:B = 2:1, (b) Ta:B = 3:2, (c) Ta:B = 5:6, and (d) Ta:B = 3:4.

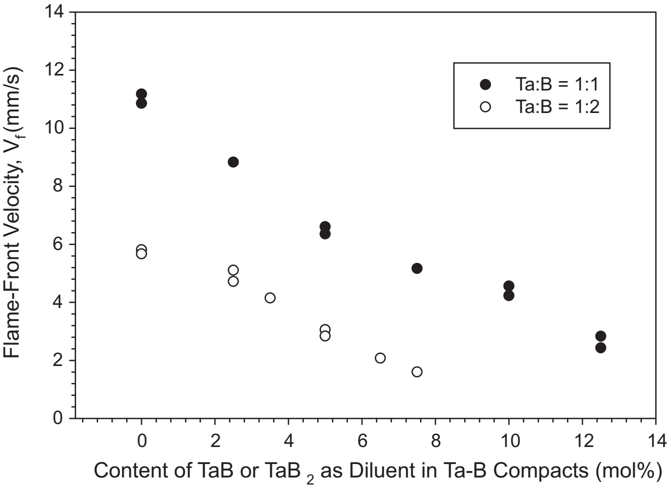

Fig. 6. Effects of molar contents of TaB and $TaB_2$ as diluents on flame-front velocity of powder compacts with Ta:B = 1:1 and 1:2.

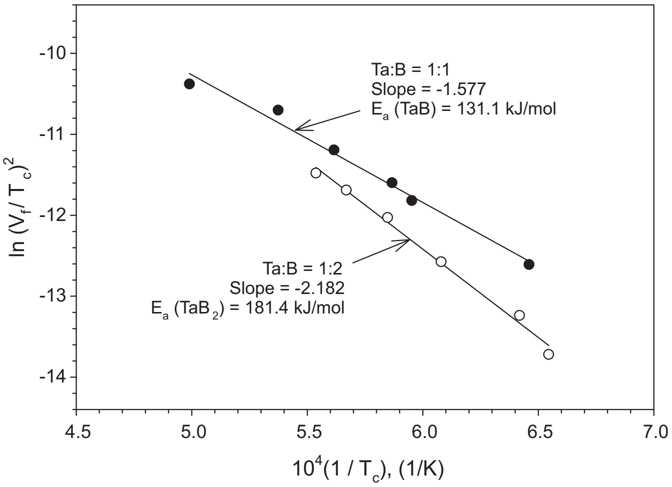

Fig. 7. Relations between flame-front velocity and combustion temperature for determination of activation energies of TaB and $TaB_2$ by combustion synthesis.

phases to be formed by solid state combustion. It is interesting to note that an almost identical result was observed in combustion synthesis of the Nb–B compounds, indicating no formation of $Nb_3B_2$ and $Nb_5B_6$ in the final products [20].

### 3.3. Determination of activation energy

In view of the formation of single-phase TaB and $TaB_2$ from solid state combustion, it is highly instructive to deduce the activation energy for these two SHS processes on the basis of the flame-front velocity and combustion temperature. The apparent activation energy of the solid-phase reaction is generally determined by realizing the dependence of the reaction front velocity on combustion temperature. Such a relationship can be expressed in the following simplified form [20,27].

$$\left(\frac{V_f}{T_c}\right)^2 = f(n)\left(\frac{R}{E_a}\right)K\exp\left(-\frac{E_a}{RT_c}\right) \tag{1}$$

where $V_f$ is the flame-front propagation velocity, $T_c$ the combustion front temperature, $E_a$ the activation energy of the reaction, $R$ the universal gas constant, $f(n)$ a function of the kinetic order of the reaction, and $K$ a constant which accounts for the heat capacity of the product, the thermal conductivity, and the heat of reaction. According to Eq. (1), the slope of a straight line correlating $\ln(V_f/T_c)^2$ versus $1/T_c$ can provide the apparent activation energy of the reaction.

The relative change in the reaction front velocity with respect to combustion temperature can be established by diluting the reactant mixture to different extents. As suggested by Bertolino et al. [27], TaB and $TaB_2$ synthesized in this study are the most suitable diluents for the powder mixtures of Ta:B = 1:1 and 1:2, respectively. The subsequent results are reported in Fig. 6, showing that in the case of Ta:B = 1:1 the flame-front velocity decreases from 11.2 mm/s for the undiluted sample to 2.43 mm/s for the 12.5 mol% TaB-diluted sample. The combustion temperature decreased correspondingly from 1732 to 1275 °C, which was plotted inversely as the abscissa in Fig. 7.

Due to the weaker reaction exothermicity for the sample of Ta:B = 1:2 compared to that of Ta:B = 1:1, the maximum content of $TaB_2$ as the diluent in the powder mixture was reduced to 7.5 mol%. With increasing $TaB_2$ content, Fig. 6 indicates that the combustion front velocity decreases from 5.8 to 1.6 mm/s. The associated combustion temperature decreases from 1533 to 1255 °C. Based upon the measured data, Fig. 7 presents two best-fitted lines correlating $\ln(V_f/T_c)^2$ versus $1/T_c$ for the cases of Ta:B = 1:1 and 1:2. The apparent activation energies for the synthesis of TaB and $TaB_2$ by solid state combustion were then determined as 131.1 and 181.4 kJ/mol, respectively.

According to Kashireninov et al. [28] and Kurbatkina et al. [29], the combustion mechanism of the Ta–B system could be substantially affected by the presence of boron oxide ($B_2O_3$) on the boron particles. It has been proposed [29] that the reaction in the combustion wave is preceded by the melting of $B_2O_3$ at 723 K. Subsequent dissolution of solid boron into the molten $B_2O_3$ layer results in the formation of volatile suboxide $B_2O_2$, which acts as the carrier of boron to Ta. This means that oxygen present in the oxide layer plays a role as the transport agent for mass transfer of boron [28,29]. It is believed that such a gas-phase transport process governs self-sustaining combustion of the Ta–B system and is responsible for the relatively low activation energy about 130–180 kJ/mol for SHS formation of TaB and $TaB_2$. As a result, the sequence of phase transformation is initiated by the production of TaB from the reaction of Ta with $B_2O_2$ and followed by the formation of $Ta_3B_4$ and then $TaB_2$ through successive interaction with boron.

## 4. Conclusions

This study represents the first attempt to investigate the feasibility of producing specific tantalum borides (including $Ta_2B$, $Ta_3B_2$, TaB, $Ta_5B_6$, $Ta_3B_4$, and $TaB_2$) from the elemental powder compacts with their corresponding stoichiometries by combustion synthesis in the SHS mode. Solid state combustion of the Ta–B sample was characterized by a nearly planar reaction front propagating in a self-sustaining manner. The starting stoichiometry of the reactant compact played an important role in combustion characteristics as well as in the phase constituent of the final product. With the increase of the content of boron in the sample from the proportion of Ta:B = 2:1 to 1:2, the combustion temperature increased, reached a peak value at Ta:B = 1:1, and then decreased. Consequently, the variation of reaction front velocity with sample composition was in a manner consistent with that of combustion temperature.

Among six borides of tantalum, TaB and $TaB_2$ are the only two phases produced in the pure form through solid state combustion of constituent elements. Based upon the temperature dependence of combustion wave velocity observed in this study, the activation energies for formation of TaB and $TaB_2$ by the SHS reactions were deduced to be 131.1 and 181.4 kJ/mol, respectively. In contrast, $Ta_3B_2$ and $Ta_5B_6$ were considered as kinetically unfavorable phases, because they did not appear in any synthesized products. For the Ta-rich samples of Ta:B = 2:1 and 3:2, their resulting products contained two boride phases, $Ta_2B$ and TaB, along with a large amount of unreacted Ta. The final products obtained from boron-rich samples of Ta:B = 5:6 and 3:4 were composed of three boride phases TaB, $TaB_2$, and $Ta_3B_4$.

## Acknowledgement

This research was sponsored by the National Science Council of Taiwan, ROC, under the grants of NSC 98-2221-E-035-065-MY2.

## References

[1] R.G. Munro, Material properties of titanium diboride, J. Res. Natl. Inst. Stand. Technol. 105 (2000) 709–720.

[2] W.G. Fahrenholtz, G.E. Hilmas, I.G. Talmy, J.A. Zaykoski, Refractory diborides of zirconium and hafnium, J. Am. Ceram. Soc. 90 (5) (2007) 1347–1364.

[3] S.Q. Guo, Densification of $ZrB_2$-based composites and their mechanical and physical properties: a review, J. Eur. Ceram. Soc. 29 (2009) 995–1011.

[4] X. Zhang, G.E. Hilmas, W.G. Fahrenholtz, Synthesis, densification, and mechanical properties of $TaB_2$, Mater. Lett. 62 (2008) 4251–4253.

[5] E. Bilgi, H.E. Camurlu, B. Akgun, Y. Topkaya, N. Sevinc, Formation of $TiB_2$ by volume combustion and mechanochemical process, Mater. Res. Bull. 43 (2008) 873–881.

[6] R. Licheri, R. Orrù, C. Musa, A.M. Locci, G. Cao, Consolidation via spark plasma sintering of $HfB_2$/SiC and $HfB_2$/HfC/SiC composite powders obtained by self-propagating high-temperature synthesis, J. Alloys Compd. 478 (2010) 572–578.

[7] T.B. Massalski, H. Okamoto, P.R. Subramanian, L. Kacprzak (Eds.), Binary Alloy Phase Diagrams, ASM International Materials Park, OH, USA, 1996.

[8] H. Bolmgren, T. Lundström, L.E. Tergenius, S. Okada, I. Higashi, The crystal structure of $Ta_5B_6$, J. Less Comm. Met. 161 (1990) 341–345.

[9] I. Hideaki, S. Yusuke, K. Satoshi, N. Shigeharu, Synthesis of tantalum boride powder by solid state reaction and its sintering, J. Ceram. Soc. Jpn. 98 (1990) 264–268.

[10] P. Peshev, L. Leyarovska, G. Bliznakov, On the borothermic preparation of some vanadium, niobium, and tantalum borides, J. Less Comm. Met. 15 (1968) 259–267.

[11] A.G. Merzhanov, Combustion processes that synthesize materials, J. Mater. Process. Technol. 56 (1996) 222–241.

[12] Z.A. Munir, U. Anselmi-Tamburini, Self-propagating exothermic reactions: the synthesis of high-temperature materials by combustion, Mater. Sci. Rep. 3 (1989) 277–365.

[13] P. Mossino, Some aspects in self-propagating high-temperature synthesis, Ceram. Int. 30 (2004) 311–332.

[14] C.L. Yeh, Combustion synthesis involving thermite reactions, in: M. Lackner (Ed.), Combustion Synthesis – Novel Routes to Novel Materials, Bentham Science, 2010.

[15] A.G. Merzhanov, I.P. Borovinskaya, Self-propagated high-temperature synthesis of refractory inorganic compounds, Dokl. Akad. Nauk USSR 204 (1972) 366–369.

[16] I.P. Borovinskaya, A.G. Merzhanov, N.P. Novikov, A.K. Filonenko, Gasless combustion of mixtures of powdered transition metals with boron, Combust. Explos. Shock Waves 10 (1974) 2–10.

[17] J.B. Holt, D.D. Kingman, G.M. Bianchini, Kinetics of the combustion synthesis of $TiB_2$, Mater. Sci. Eng. 71 (1985) 321–327.

[18] S. Nakane, T. Endo, K. Hirota, Simultaneous synthesis and densification of $\alpha$-Zr(N)/$ZrB_2$ composites by self-propagating high-temperature combustion under high nitrogen pressure, Ceram. Int. 35 (2009) 2145–2149.

[19] C.L. Yeh, W.H. Chen, Preparation of niobium borides NbB and $NbB_2$ by self-propagating combustion synthesis, J. Alloys Compd. 420 (2006) 111–116.

[20] C.L. Yeh, W.H. Chen, A comparative study on combustion synthesis of Nb–B compounds, J. Alloys Compd. 422 (2006) 78–85.

[21] C.L. Yeh, Y.L. Chen, Combustion synthesis of TiC–$TiB_2$ composites, J. Alloys Compd. 463 (2008) 373–377.

[22] C.L. Yeh, Y.L. Chen, An experimental study on self-propagating high-temperature synthesis in the Ta–$B_4C$ system, J. Alloys Compd. 478 (2009) 163–167.

[23] R. Licheri, R. Orrù, C. Musa, G. Cao, Synthesis, densification and characterization of $TaB_2$–SiC composites, Ceram. Int. 36 (2010) 937–941.

[24] P. Shen, W. Sun, B. Zou, L. Zhan, Q. Jiang, Al content dependence of reaction behaviors and mechanism in combustion synthesis of $TiB_2$–AlN-based composites, Chem. Eng. J. 150 (2009) 261–268.

[25] C.L. Yeh, R.F. Li, Formation of $TiB_2$–$Al_2O_3$ and $NbB_2$–$Al_2O_3$ composites by combustion synthesis involving thermite reactions, Chem. Eng. J. 147 (2009) 405–411.

[26] Z.I. Zaki, Combustion synthesis of mullite–titanium boride composite, Ceram. Int. 35 (2009) 673–678.

[27] N. Bertolino, U. Anselmi-Tamburini, F. Maglia, G. Spinolo, Z.A. Munir, Combustion synthesis of Zr–Si intermetallic compounds, J. Alloys Compd. 288 (1999) 238–248.

[28] O.E. Kashireninov, I.A. Yuranov, A.A. Fomin, High-temperature thermochemistry of gas-phase transport in solid state combustion of SHS-systems, in: Proc. 24th Symposium (International) on Combustion, The Combustion Institute, 1992, pp. 1899–1906.

[29] V.V. Kurbatkina, E.A. Levashov, E.I. Patsera, N.A. Kochetov, A.S. Rogachev, Combustion and structure formation in the mechanoactivated Cr–B system, Int. J. Self-Propagating High-Temperature Synth. 17 (2008) 189–194.